Sensors and Materials, Vol. 38, No. 2 (2026) 509–514
MYU Tokyo

S & M 4313

Scintillation and Dosimetric Properties of $KHSi_2O_5$ Single Crystals Fabricated by the Hydrothermal Method

Haruaki Ezawa,* Takumi Kato, Daisuke Nakauchi,
Noriaki Kawaguchi, and Takayuki Yanagida

Nara Institute of Science and Technology (NAIST), Ikoma, Nara 630-0192, Japan

(Received October 17, 2025; accepted November 7, 2025)

Keywords: hydrothermal method, single crystals, Tb, scintillation, thermally stimulated luminescence

Undoped and 0.1% Tb-doped $KHSi_2O_5$ single crystals were synthesized by the hydrothermal method, and their scintillation and dosimetric properties were systematically investigated. The scintillation spectra of the Tb-doped $KHSi_2O_5$ single crystal exhibited an emission peak at 330 nm originating from the host material and additional peaks in the 490–620 nm range, corresponding to the 4f–4f transitions of Tb^{3+} ions. The thermally stimulated luminescence (TSL) glow curves showed two peaks at approximately 80 and 300 °C for all the Tb-doped samples. In the TSL dose response of the Tb-doped sample, the lowest detectable dose was 30 mGy, and a linear dose response was observed over the dose range of 30–3000 mGy.

1. Introduction

Luminescent materials are used in ionizing radiation detectors to convert invisible radiation into visible photons. Among them, scintillators are the best known, as they convert a single high-energy ionizing event into thousands of ultraviolet–visible photons almost instantaneously.(1–12) Because of these properties, scintillators have found extensive applications in high-energy physics, well logging, security screening, and medical imaging.(12–15)

In contrast, storage-type phosphors can trap a portion of the absorbed radiation energy and subsequently release it upon external stimulation.(16,17) Such materials are used in personal dosimetry and in imaging plates for medical and dental X-ray applications.(18–22) Upon exposure to radiation, electron–hole pairs are generated and trapped at the trapping centers. When thermally or optically stimulated, the trapped carriers are released and recombined at luminescence centers, emitting luminescence. The emissions triggered by thermal and optical stimulations are referred to as thermally stimulated luminescence (TSL) and optically stimulated luminescence (OSL), respectively.(23–27) For personal dosimetry, storage-type phosphors are required to have (i) an effective atomic number (Z_{eff}) close to that of soft human tissue (Z_{eff} = 7.29), (ii) a wide dynamic range, (iii) high luminescence intensity, (iv) low signal fading, and (v) a linear relationship between irradiation dose and luminescence intensity.(17,28) However, no

*Corresponding author: e-mail: ezawa.haruaki.ec6@ms.naist.jp
https://doi.org/10.18494/SAM5990

ISSN 0914-4935
https://myukk.org/

existing storage-type phosphor satisfies all of these requirements simultaneously; therefore, the development of new materials remains necessary.

Although the Z_{eff} (14) of $KHSi_2O_5$ is nearly twice that of soft human tissue, it is comparable to that of commercial thermoluminescent dosimeters (TLDs).(28) Therefore, $KHSi_2O_5$ can be regarded as a potential dosimetric material. To the best of our knowledge, however, there are no reports on the TSL properties of $KHSi_2O_5$. In this work, Tb^{3+} ions were chosen as luminescence centers because their emission wavelengths well match the spectral sensitivities of common photodetectors, including photodiodes and photomultiplier tubes.(29) Accordingly, undoped and Tb-doped $KHSi_2O_5$ single crystals were grown by the hydrothermal method, and their scintillation and dosimetric properties were systematically investigated.

2. Materials and Methods

Different concentrations of Tb (0 and 0.1% relative to SiO_2) were doped into the host material. The undoped and 0.1% Tb-doped $KHSi_2O_5$ single crystals were synthesized by the hydrothermal method. SiO_2 and Tb_4O_7 were used as starting materials and thoroughly mixed. The mixed materials (0.4 g) and 30 mol% KOH solution (0.4 ml) were placed in a silver tube (7 cm in length). The silver tube was sealed and set in a hydrothermal furnace to grow the single crystals. The reaction was carried out at 650 °C under a pressure of 150 MPa for 24 h, followed by slow cooling to 350 °C at a rate of 25 °C for 12 h.

The energy-dispersive X-ray spectroscopy (EDX) spectra of the fabricated samples were measured using a scanning electron microscope (JEOL, JCM-6000Plus). The fabricated samples were ground using a mortar and pestle. The obtained powder was used for powder X-ray diffraction (XRD) measurements using an X-ray diffractometer (Rigaku, MiniFlex600). The remaining samples, which were not used for powder XRD measurements, were used to evaluate the scintillation and dosimetric properties.

X-ray-induced scintillation spectra were measured using our original equipment under a bias voltage of 40 kV and a tube current of 1.2 mA.(30) TSL glow curves were evaluated using a temperature controller/power supply (SCR-SHQ-A, Sakaguchi E.H Voc), a photomultiplier tube (Hamamatsu, H11890-01), and the above diffractometer as the X-ray source.(31) For the TSL dose response measurements, the temperature controller/power supply, a Si CCD-based spectrometer, and an X-ray generator (Spellman, XRB80P&N200X4550) were used. The X-ray irradiated the sample under the conditions of 40 kV for the bias voltage and a range of 0.052–5.2 mA for the tube current. The $KHSi_2O_5$ single crystals were heated to 300 °C at a rate of 1 °C /s to perform the TSL measurements.

3. Results and Discussion

The EDX spectra of the undoped and 0.1% Tb-doped $KHSi_2O_5$ samples are shown in Fig. 1. The chemical composition of the undoped sample was O: 40.65 at%, Si: 46.32 at%, and K: 13.03 at%, with Ag not detected (ND). For the 0.1% Tb-doped sample, the composition was O: 42.44 at%, Si: 44.04 at%, K: 13.49 at%, Ag: ND, and Tb: 0.03 at%. The results confirm that no Ag contamination originating from the silver tube occurred during the hydrothermal synthesis.

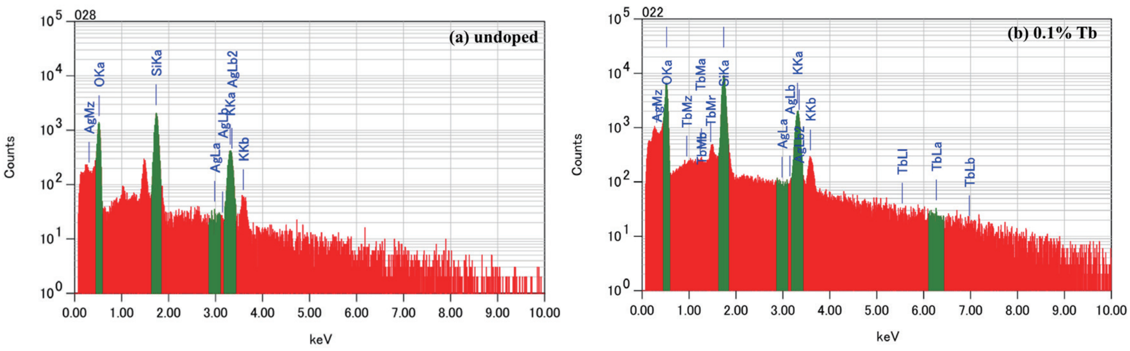

(a) (b)

Fig. 1. (Color online) EDX spectra of (a) undoped and (b) 0.1% Tb-doped samples.

The powder XRD patterns of the fabricated samples, together with reference data (ICSD 23516), are shown in Fig. 2. The insets show the photographs of the fabricated $KHSi_2O_5$ single crystals. The thicknesses of the undoped and Tb-doped samples were approximately 1.3 and 0.9 mm, respectively. The diffraction patterns of the prepared samples matched well with reference data, and no additional peaks were observed, indicating that single-phase $KHSi_2O_5$ crystals were successfully obtained. The $KHSi_2O_5$ phase crystallized in the orthorhombic structure with space group Pmnb (62). Some of the diffraction peaks in the observed patterns exhibited high intensities corresponding to the (h k l) planes of (0 2 0), (0 3 1), (0 8 0), and (1 4 0) at around 2θ = 14.11, 28.39, 58.87, and 30.53°, respectively.

The X-ray-induced scintillation spectra of the fabricated $KHSi_2O_5$ single crystals are shown in Fig. 3. Both the undoped and Tb-doped $KHSi_2O_5$ single crystals exhibited a broad emission peak at around 340 nm, which was attributed to the host material. In addition, the Tb-doped $KHSi_2O_5$ single crystal exhibited sharp emission peaks at 490, 550, 580, and 620 nm, corresponding to the $^5D_4 \rightarrow {}^7F_6$, $^5D_4 \rightarrow {}^7F_5$, $^5D_4 \rightarrow {}^7F_4$, and $^5D_4 \rightarrow {}^7F_3$ transitions of Tb^{3+} ions, respectively.(22,29,32–35)

The TSL glow curves of the fabricated samples are presented in Fig. 4. Two TSL glow peaks were observed at approximately 70 and 170 °C in the undoped $KHSi_2O_5$ single crystal. In the Tb-doped $KHSi_2O_5$ single crystal, a single peak was observed at approximately 90 °C. The TSL intensity of each sample was determined by normalizing the peak intensity of the TSL glow curve to the sample mass. The TSL intensity of the Tb-doped $KHSi_2O_5$ single crystal was higher than that of the undoped $KHSi_2O_5$ single crystal.

The TSL dose response functions of undoped and Tb-doped $KHSi_2O_5$ single crystals are shown in Fig. 5. The TSL intensity was defined as the integrated area under the glow curve. The X-ray irradiation range in this experiment was 0.01–1000 mGy, which corresponds to the range over which the X-ray generator could accurately deliver the dose. For the undoped sample, the lowest detectable dose was 100 mGy, and the TSL signal exhibited a linear response in the range of 100–3000 mGy. For the Tb-doped sample, the lowest detectable dose was 30 mGy, and the TSL signal exhibited a linear response in the range of 30–3000 mGy. Furthermore, dose linearity was determined using the formula $y = e^a x^b$ (x and y are X-ray dose and TSL intensity, respectively) and $|r|$ values. In the previous study, the detection limit of a commercially available

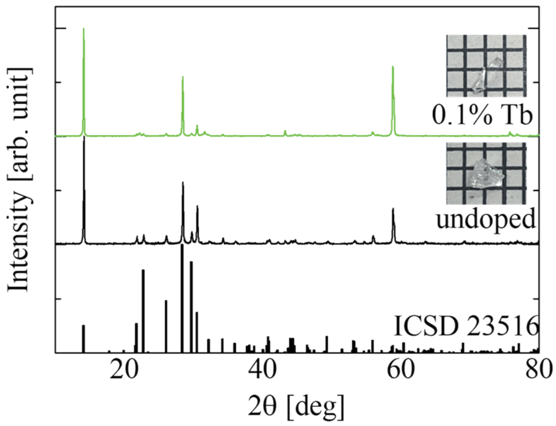

Fig. 2. (Color online) XRD patterns of undoped and Tb-doped samples and reference data (ICSD 23516). The insets indicate photographs of the fabricated samples.

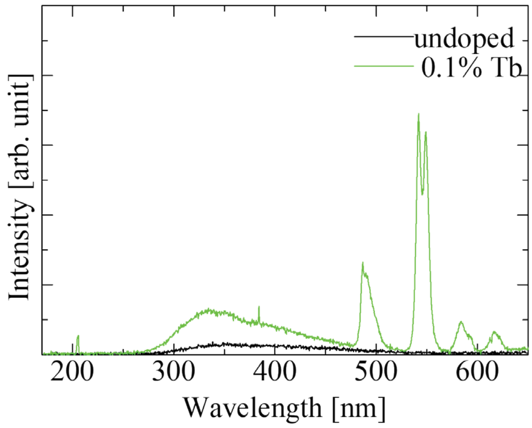

Fig. 3. (Color online) X-ray-induced scintillation spectra of undoped and Tb-doped samples.

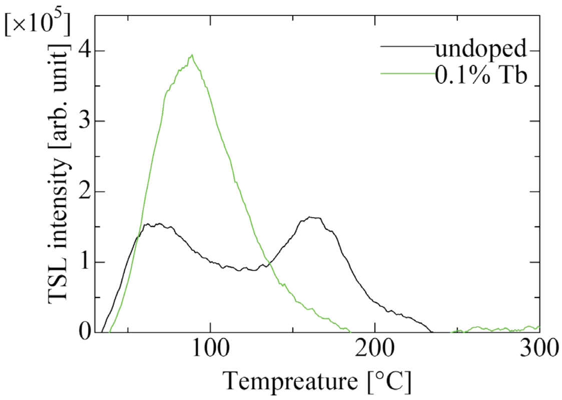

Fig. 4. (Color online) TSL glow curves of fabricated samples after 100 Gy X-ray exposure.

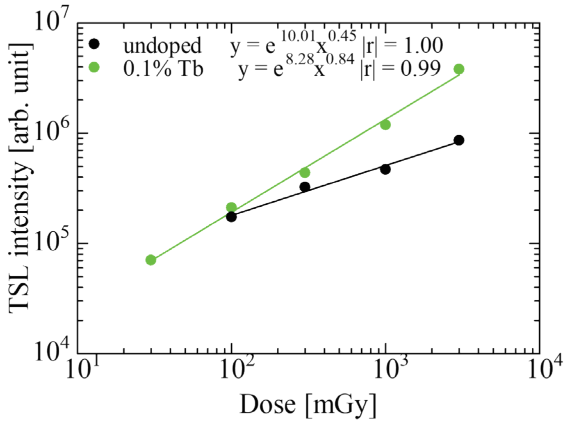

Fig. 5. (Color online) TSL dose response functions of undoped and Tb-doped samples.

Mg, Ti-doped LiF product was 0.02 mGy.(36) In comparison, the detection limit of the Tb-doped $KHSi_2O_5$ single crystal was determined to be 30 mGy, indicating that its sensitivity is lower than that of the commercially available product.

4. Conclusions

Undoped and Tb-doped $KHSi_2O_5$ single crystals were successfully fabricated by the hydrothermal method. From PXRD patterns, the fabricated samples were confirmed to be single-phase $KHSi_2O_5$. In scintillation spectra, an emission peak at around 340 nm was observed and attributed to the host material. In the Tb-doped $KHSi_2O_5$ single crystal, additional emission peaks at 490, 550, 580, and 620 nm were observed, which were due to the 4f–4f transitions of

Tb^{3+} ions. The TSL glow peaks were observed at 70 and 170 °C for the undoped $KHSi_2O_5$ single crystal and 90°C for the Tb-doped $KHSi_2O_5$ single crystal. From the TSL dose response function, the lowest detectable dose of the Tb-doped $KHSi_2O_5$ single crystal was estimated to be 30 mGy.

Acknowledgments

This work was supported by JSPS KAKENHI (22H00309, 23K25126, 24K03197, 23K13689, and 25K08266), the Cooperative Research Project of Research Center for Biomedical Engineering, and JST SPRING, Japan Grant Number JPMJSP2140.

References

1 T. Yanagida, K. Okazaki, K. Miyajima, T. Kato, D. Nakauchi, and N. Kawaguchi: Sens. Mater. **37** (2025) 453. https://doi.org/10.18494/SAM5423
2 K. Miyajima, A. Nishikawa, T. Kato, D. Nakauchi, N. Kawaguchi, and T. Yanagida: Sens. Mater. **37** (2025) 481. https://doi.org/10.18494/SAM5436
3 H. Fukushima, R. Tsubouchi, T. Matsuura, T. Yoneda, and T. Yanagida: Sens. Mater. **37** (2025) 487. https://doi.org/10.18494/SAM5438
4 S. Otake, S. Takase, T. Kato, D. Nakauchi, N. Kawaguchi, and T. Yanagida: Sens. Mater. **37** (2025) 519. https://doi.org/10.18494/SAM5433
5 M. Koshimizu, K. Tanahashi, Y. Fujimoto, and K. Asai: Sens. Mater. **37** (2025) 539. https://doi.org/10.18494/SAM5448
6 D. Nakauchi, T. Kato, N. Kawaguchi, and T. Yanagida: Sens. Mater. **37** (2025) 547. https://doi.org/10.18494/SAM5425
7 K. Ichiba, K. Watanabe, K. Okazaki, T. Kato, D. Nakauchi, N. Kawaguchi, and T. Yanagida: Sens. Mater. **37** (2025) 553. https://doi.org/10.18494/SAM5426
8 T. Kunikata, K. Okazaki, H. Kimura, S. Takase, T. Kato, D. Nakauchi, N. Kawaguchi, and T. Yanagida: Sens. Mater. **37** (2025) 563. https://doi.org/10.18494/SAM5428
9 N. Kawaguchi, K. Yamabayashi, K. Okazaki, R. Takahashi, T. Kato, D. Nakauchi, and T. Yanagida: Sens. Mater. **37** (2025) 617. https://doi.org/10.18494/SAM5479
10 T. Yanagida, T. Kato, D. Nakauchi, and N. Kawaguchi: Sens. Mater. **36** (2024) 443. https://doi.org/10.18494/SAM4748
11 T. Kunikata, P. Kantuptim, D. Shiratori, T. Kato, D. Nakauchi, N. Kawaguchi, and T. Yanagida: Sens. Mater. **36** (2024) 457. https://doi.org/10.18494/SAM4754
12 K. Ichiba, T. Kato, D. Nakauchi, N. Kawaguchi, and T. Yanagida: Sens. Mater. **36** (2024) 451. https://doi.org/10.18494/SAM4752
13 D. Shiratori, A. Masuno, T. Kato, Y. Fukuchi, and T. Yanagida: Sens. Mater. **37** (2025) 497. https://doi.org/10.18494/SAM5439
14 S. Muneta, N. Kawano, D. Nakauchi, T. Kato, K. Okazaki, K. Ichiba, T. Kunikata, A. Nishikawa, K. Miyazaki, F. Kagaya, K. Shinozaki, and T. Yanagida: Sens. Mater. **37** (2025) 509. https://doi.org/10.18494/SAM5441
15 K. Miyazaki, D. Nakauchi, Y. Takebuchi, T. Kato, N. Kawaguchi, and T. Yanagida: Sens. Mater. **37** (2025) 575. https://doi.org/10.18494/SAM5430
16 H. Fujiwara, T. Negishi, L. Takahashi, and K. Shinsho: Sens. Mater. **37** (2025) 463. https://doi.org/10.18494/SAM5475
17 T. Kato, A. Nishikawa, D. Nakauchi, N. Kawaguchi, and T. Yanagida: Sens. Mater. **37** (2025) 475. https://doi.org/10.18494/SAM5424
18 H. Ezawa, T. Kato, Y. Takebuchi, K. Okazaki, K. Ichiba, D. Nakauchi, N. Kawaguchi, and T. Yanagida: Sens. Mater. **37** (2025) 581. https://doi.org/10.18494/SAM5431
19 H. Kimura, T. Fujiwara, H. Kato, M. Koshimizu, G. Wakabayashi, Y. Takebuchi, T. Kato, D. Nakauchi, N. Kawaguchi, and T. Yanagida: Sens. Mater. **37** (2025) 599. https://doi.org/10.18494/SAM5442
20 K. Yamabayashi, K. Okazaki, D. Nakauchi, T. Kato, N. Kawaguchi, and T. Yanagida: Sens. Mater. **37** (2025) 627. https://doi.org/10.18494/SAM5434

21 M. Koshimizu, K. Oba, Y. Fujimoto, and K. Asai: Sens. Mater. **36** (2024) 565. https://doi.org/10.18494/SAM4761
22 H. Ezawa, Y. Takebuchi, T. Kato, D. Nakauchi, N. Kawaguchi, and T. Yanagida: Jpn J Appl Phys **62** (2023) 122001. https://doi.org/10.35848/1347-4065/ad0a46
23 Y. Takebuchi, M. Morioka, Y. Nakashima, K. Tezuka, H. Kimura, S. Otake, and T. Yanagida: Sens. Mater. **37** (2025) 525. https://doi.org/10.18494/SAM5437
24 K. Okazaki, M. Koshimizu, D. Nakauchi, Y. Takebuchi, K. Ichiba, H. Ezawa, T. Kato, N. Kawaguchi, and T. Yanagida: Sens. Mater. **37** (2025) 557. https://doi.org/10.18494/SAM5427
25 A. Nishikawa, K. Ichiba, T. Kato, D. Nakauchi, N. Kawaguchi, and T. Yanagida: Sens. Mater. **37** (2025) 569. https://doi.org/10.18494/SAM5429
26 R. Tsubouchi, H. Fukushima, T. Kato, D. Nakauchi, S. Saijo, T. Matsuura, N. Kawaguchi, T. Yoneda, and T. Yanagida: Sens. Mater. **36** (2024) 481. https://doi.org/10.18494/SAM4763
27 D. Shiratori, H. Kimura, Y. Fukuchi, and T. Yanagida: Sens. Mater. **36** (2024) 547. https://doi.org/10.18494/SAM4764
28 A. Fujii, K. Miyazaki, T. Kato, D. Nakauchi, N. Kawaguchi, and T. Yanagida: Solid State Sci. **168** (2025) 108013. https://doi.org/10.1016/j.solidstatesciences.2025.108013
29 H. Ezawa, Y. Takebuchi, K. Okazaki, T. Kato, D. Nakauchi, N. Kawaguchi, and T. Yanagida: Sens. Mater. **36** (2024) 465. https://doi.org/10.18494/SAM4757
30 T. Yanagida, K. Kamada, Y. Fujimoto, H. Yagi, and T. Yanagitani: Opt. Mater. **35** (2013) 2480. https://doi.org/10.1016/j.optmat.2013.07.002
31 G. Okada, T. Kato, D. Nakauchi, K. Fukuda, and T. Yanagida: Sens. Mater. **28** (2016) 897. https://doi.org/10.18494/SAM.2016.1357
32 R. Takahashi, K. Okazaki, D. Nakauchi, T. Kato, N. Kawaguchi, and T. Yanagida: Sens. Mater. **37** (2025) 593. https://doi.org/10.18494/SAM5435
33 H. Kimura, H. Fukushima, K. Watanabe, T. Fujiwara, H. Kato, M. Tanaka, T. Kato, D. Nakauchi, N. Kawaguchi, and T. Yanagida: Sens. Mater. **36** (2024) 507. https://doi.org/10.18494/SAM4767
34 H. Ezawa, Y. Takebuchi, K. Ichiba, T. Kato, D. Nakauchi, N. Kawaguchi, and T. Yanagida: Opt. Mater. **147** (2024) 114665. https://doi.org/10.1016/j.optmat.2023.114665
35 E. Haruaki, Y. Takebuchi, K. Okazaki, K. Ichiba, T. Kato, D. Nakauchi, N. Kawaguchi, and T. Yanagida: Radiat. Phys. Chem. **220** (2024) 111721. https://doi.org/10.1016/j.radphyschem.2024.111721
36 P. Bilski: Radiat Prot Dosimetry **100** (2002) 199. https://doi.org/10.1093/oxfordjournals.rpd.a005847